

Craniofacial architectural constraints and their importance for reconstructing the early *Homo* skull KNM-ER 1470

Timothy G. Bromage* / James M. McMahon ** / J. Francis Thackeray *** / Ottmar Kullmer**** /
 Russell Hogg ***** / Alfred L. Rosenberger***** / Friedemann Schrenk***** /
 Donald H. Enlow*****

Objective: Our objective is to exploit architectural constraint for the analysis and interpretation of craniofacial form, which we apply here to the reconstruction of the early *Homo* cranium KNM-ER 1470. We are motivated to perform this study because in the absence of biological criteria our preconceptions are likely to govern our concept of craniofacial form. **Study Design:** We reassembled the fragmented parts—left and right halves of the calvaria and the face—according to mammalian craniofacial architectural constraints described by Donald H. Enlow and colleagues. **Results:** When evaluated on a biological premise, KNM-ER 1470 is found to have a more prognathic midface than commonly appreciated. The relationship between facial prognathism and cranial capacity also provides an estimate downward for this specimen, from 752cc to ca. 700cc. **Conclusion:** Awareness of our preconceptions is critical to the performance of relatively unbiased research in fields characterized by interpretations of morphology. When perceptual bias is relatively minimized, applied here as an architecturally constrained of KNM-ER 1470 craniofacial skeleton, we are able to provide the scientific community with a more tractable Gestalt perspective of form.

Keywords: KNM-ER 1470, craniofacial architecture, developmental constraint
 J Clin Pediatr Dent 33(1): 43–54, 2008

INTRODUCTION

Fragments of the craniofacial skeleton known as KNM-ER 1470 were discovered in 1972 from Late Pliocene deposits east of Lake Turkana, northern Kenya,^{1,2}

which articulated to produce 3 main parts: left and right calvaria elements and facial skeleton. Controversy immediately surrounded the specimen, which has been the subject of considerable reflection on scientific conduct and demeanor in paleoanthropology.^{3,5} Briefly, the initial clamor centered most of all on its purported age of nearly 3 million years, a radiometric age determination that did not agree with biochronological evidence. To this was added disagreement amongst its describers about whether the specimen was representative of the genus *Australopithecus* or of *Homo*; a review of opinions may be found in Wood.⁶

Following discovery of the many fragments associated with KNM-ER 1470, its reassembly by Richard and Meave Leakey, Michael Day, and Alan Walker began at the Koobi Fora base camp. Fragments that were felt to be unambiguously matched ultimately came together to form left and right calvaria elements, which materialized into what was regarded as a relatively large brain. The view prevailing at that time, namely that a large brain would associate with a small and vertically disposed facial skeleton, led to the assembled facial skeleton ultimately being depicted as such.⁷

This reconstruction was promulgated for and presented to the lay science press for purposes of announcing the discovery of KNM-ER 1470 and highlighting hominin diversity at Koobi Fora.^(e.g. 8) However, in the professional literature, prudence was favored:⁴

The face is less complete and although there are

* Timothy G. Bromage Ph.D., Departments of Biomaterials & Biomimetics and Basic Science & Craniofacial Biology, New York University College of Dentistry
 ** James M. McMahon Ph.D., University of Rochester Medical Center, School of Nursing
 *** J. Francis Thackeray Ph.D., Department of Palaeontology and Palaeoenvironmental Studies, Transvaal Museum
 **** Ottmar Kullmer Ph.D., Department of Paleoanthropology, Senckenberg Forschungsinstitut und Naturmuseum
 ***** Russell Hogg Ph.D. candidate, Department of Anthropology, The Graduate Center, City University of New York
 ***** Alfred L. Rosenberger Ph.D., Department of Anthropology and Archaeology, Brooklyn College, City University of New York
 ***** Friedemann Schrenk Ph.D., Department of Paleoanthropology, Senckenberg Forschungsinstitut und Naturmuseum
 ***** Donald H. Enlow Ph.D., Case School of Dental Medicine, Case Western Reserve University

Send all correspondence to: Timothy G. Bromage, Departments of Biomaterials & Basic Science, New York University College of Dentistry, 345 East 24th Street, New York, NY 10010, USA

Tel: +1 212 998-9597

Fax: +1 212 998-4445

Email: tim.bromage@nyu.edu

good contacts joining the maxilla through the face to the calvaria, many pieces are still missing. The orientation of the face is somewhat uncertain because of the distortion of the frontal base by several small, matrix filled cracks (p. 448).¹

Alan Walker recognized, however, a specific contact between assembled fragments that would lengthen the facial skeleton and make it more protrusive than was otherwise thought by the Koobi Fora team⁷:

The face was oriented “in a position that emphasized the large brain and advanced, humanlike features of the skull...but I thought this was wrong. I wanted to swing the face out at an angle, because to me 1470’s large face made it look like a big-brained australopithecine” (p. 119). “I felt, rightly or wrongly, that they were trying to squeeze the anatomy to fit their preconceived theory rather than shaping the theory to fit the anatomy” (p. 120).

While the age of KNM-ER 1470 was eventually corrected to 1.9 million years,^{9,10} a renewed effort to reconstruct the skull was first made possible by the employ of biological principles that came to light since its discovery and that are applicable to a revised Gestalt perspective.^{cf.11} These principles derive from a series of investigations by Donald H. Enlow and colleagues from the 1960’s to 1980’s. Functional anatomical boundaries of the craniofacial skeleton in humans and other mammal species were found to be characterized by important sites of growth and the relative placement of neural and pharyngeal compartments.

In this research, histological interpretations of human facial bone growth remodeling were explicitly combined with serial radiographic data in order to promote a new cephalometric system. A cephalometric system determined by actual sites of growth would, by definition, portray the underlying and developmentally constrained architectural features of the mammalian skull, as observed by the orderliness of skull ontogeny and the overwhelming similarity of facial growth across primates and other mammals.^{12,13} Enlow¹⁴ and Enlow and Hunter¹⁵ championed this new system and outlined a series of anatomical parts and counterparts which could be evaluated on the basis of growth equivalents and growth compensations between them. Facial growth was characterized by Enlow and colleagues in cephalometric applications which demonstrated a correlation between horizontal equivalents and vertical equivalents responsible for the stability and balance of craniofacial relationships.

Enlarging on this approach, Enlow *et al.*,¹⁶⁻¹⁸ Enlow and Moyers¹⁹ and Enlow²⁰ described a number of points and planes on lateral cephalographs corresponding to architectural units conforming to sites of growth, remodeling, and displacement. A procedure was developed to explain how a pattern was produced as opposed to systems of cephalomet-

ric evaluation which explained what craniofacial pattern resulted due to growth. This procedure is important in the history of developing architectural concepts because it explicitly linked dynamic growth processes to anatomical compartments and resultant craniofacial design. Bhat and Enlow²¹ subsequently noted that the part-counterpart procedure was more sensitive than traditional cephalometric methods in studies of basicranial relations to craniofacial variability because “an angular value such as basion-sella-nasion is based on midline points, none of which are involved in the actual articular fitting of basicranium, maxilla, and mandible to each other, or in the anatomic basis of bilateral positioning among the respective parts; nor do they represent growth sites directly participating in this three-part relationship” (pp. 270–272).

In 1975 Enlow and Azuma²² applied features of the new cephalometric system to investigate the prevalence of certain architectural relationships among a diversity of mammalian skulls. Their comparative sample included lateral radiographs of 116 human subjects of at least 10 years of age and 45 mammal species represented by rodents, lagomorphs, artiodactyls, carnivores and nonhuman primates. These authors defined several architectural relationships that depend on important growth sites and the developmental disposition of neural and pharyngeal matrices as follows (Fig. 1): 1) a line passing from the maxillary tuberosity (MT) through the junction of middle and anterior cranial fossae (MACF) forms the posterior maxillary (PM) plane, which is 90° to the neutral horizontal axis (NHA) of the orbit, which is between MACF and orbital midpoint (OM); 2) an average 45° angle, whose origin is the external auditory meatus (EAM), separates the MT from OM (this relationship is referred to as the meatus angle: MA); 3) the inferior base of the brain (IB), MT and prosthion (PR) are on or close to the same inferior brain-to-maxilla plane (IBMP). These relationships were found to hold for mammals in general.

However, members of the Anthroidea were found by Enlow and Azuma²² to exhibit a characteristic anterior maxillary hypoplasia (AMH), meaning that PR lay significantly

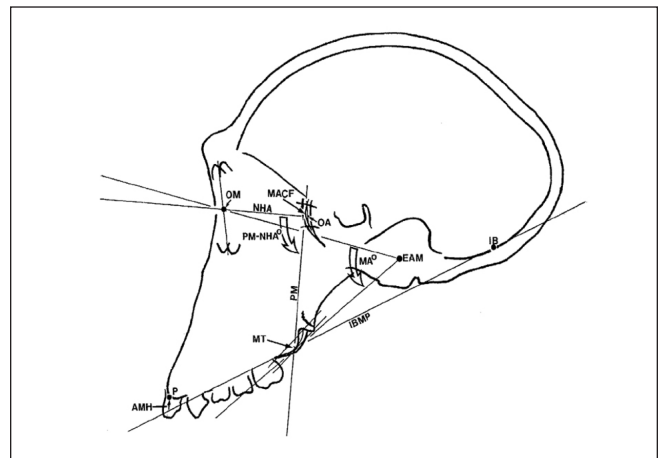


Figure 1. Craniofacial architectural landmarks, planes, and axes illustrated on the lateral headfilm tracing of a chimpanzee skull, *Pan troglodytes*.

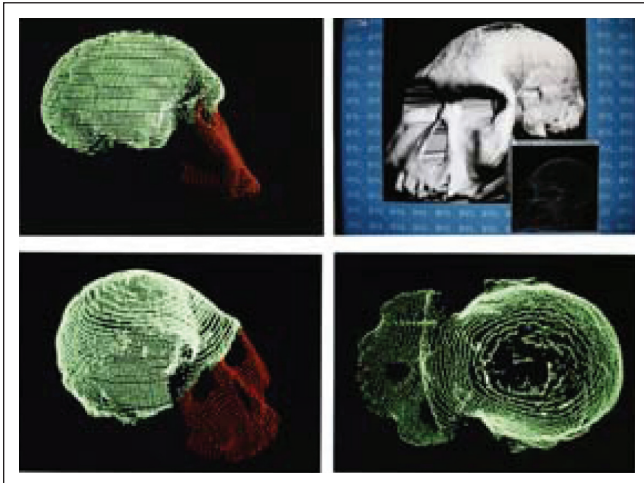


Figure 2. KNM-ER 1470 with corrected architectural hafting of the facial skeleton onto the calvaria by early laser scanning technology.

above the IBMP. Application of the architectural principles outlined by Enlow and Azuma²² were first applied to a reconstruction of KNM-ER 1470 by Bromage.¹¹ Subsequently that year two of us (TGB and ALR) undertook a laser scanning approach to repositioning the facial skeleton onto the calvaria according to these principles²³ (Fig. 2).

Bromage²⁴ subsequently tested the veracity of these relationships in an ontogenetic sample of common chimpanzees. In that study PM-NHA angles were found to remain relatively stable during growth, not significantly varying from 90°. The MA was found to be 45±3° for most individual chimpanzees, though it did tend to increase with age. A larger than 45° increase of MA was also revealed in a selection of early hominin crania, including KNM-ER 1470 when performing a 90° PM-NHA angle-based reconstruction. As noted too by Enlow and Azuma,²² the chimpanzee sample exhibited considerable AMH variability, female maxillae tending to be more hypoplastic.

Ravosa and Shea²⁵ later undertook a comparative study of Old World Monkey architectural “invariance,” which concluded that most angular constraints identified by Enlow and colleagues were too variable; this disagreement is discussed later and explored in an online Appendix to this publication. Regardless, Ravosa and Shea²⁵ did conclude that, while somewhat variable, the 90° PM-NHA angle was relatively constant in Old World Monkeys. Subsequently, Lieberman,²⁶ Lieberman and McCarthy,²⁷ and McCarthy and Lieberman²⁸ have confirmed this relationship in humans and non-human primates and employed this fact for making interpretations of the morphology, evolution, and ontogeny of craniofacial form.

There have been no concerns published on the cranial capacity of KNM-ER 1470. However, there appears to us some measure of rotational ambiguity over the calvaria articulation with the facial skeleton as there also exists between the left and right halves of the calvaria. For instance, rotating the left and right parts laterally in- or outward at their sagittal contact and in relation to each other makes a difference to the cranial capacity. Upon its initial discovery it was

thought that the KNM-ER 1470 cranial capacity would be greater than 800cc.¹ Following some reconstruction of basal portions of the endocast, however, the cranial capacity was established as 752cc.²⁹

Thackeray and Monteith³⁰ have noted a significant relationship between hominin prognathism and cranial capacity. Because the reconstruction explicitly concerns KNM-ER 1470 prognathism, the opportunity to reassess its cranial capacity is also presented here.

MATERIALS AND METHODS

Craniofacial rendering

We rendered three KNM-ER 1470 constructs for study. Virtual models of the Kenya National Museums (KNM) 3-part cast of KNM-ER 1470 were digitally acquired using both laser scanning and white light optical topometric technologies, and a flexible cast was produced, which could be deformed.

Three-dimensional models of KNM-ER 1470 were created using a Minolta Vivid 910 laser surface scanner. These laser scans were edited with Raindrop Geomagic Studio software which stores surface data as a series of polygons

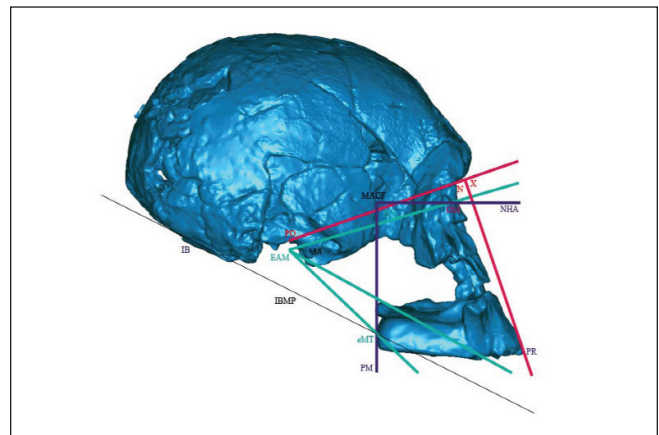


Figure 3. KNM-ER 1470 right norma lateralis laser scan with corrected architectural hafting of the facial skeleton onto the calvaria.

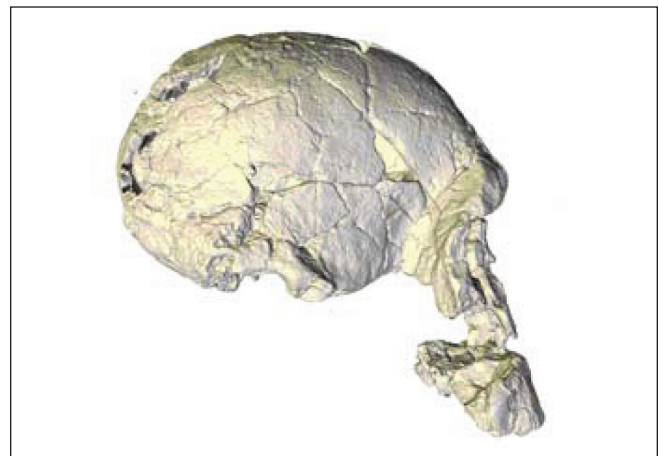


Figure 4. KNM-ER 1470 right norma lateralis optical topograph, with corrected architectural hafting of the facial skeleton onto the calvaria.

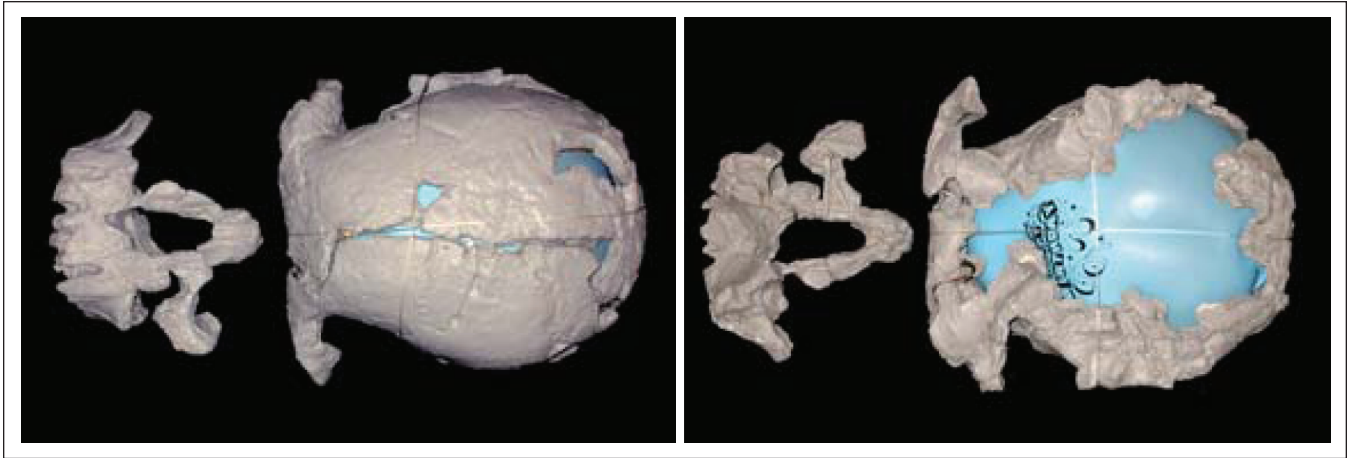


Figure 5. Superior (left) and inferior (right) views of the KNM-ER 1470 calvaria flexible cast with isolated facial part. A 675cc deformable volume has been impressed into the cranial fossae. The calvaria is being held together by nylon line.

and allows automatic alignment/registration as well as “manual” manipulation of the spatial relationships of different scans to create virtual specimens. The virtual model was rotated in coronal and translated in the transverse planes to present a *norma lateralis* projection (Fig. 3).

Optical topometry uses the known geometry between a CCD sensor, white light projector, and an observed object to mathematically triangulate x, y, and z coordinates of all line-of-sight image points. We obtained a virtual model of KNM-ER 1470 through image point superimposition and analysis of several object images obtained at different rotational positions using the “optoTOPHE” topometrical 3D-measurement system (Breuckmann GmbH, Germany) (Fig. 4). See Kullmer *et al.*³³ for details and applications of optical topometry in early hominin research.

A flexible cast was made of the Kenya National Museum 3-part cast comprising the fragmentary left and right calvaria elements and facial skeleton (Fig. 5). Each part was molded in Silastic® ERTV Silicone Rubber (Dow Corning, Midland, Michigan) according to conventional mold making methods³⁴ producing two halves with flash lines around the calvaria and facial parts in positions near to those of the original KNM-ER 1470 cast. Once cured, a vapor of silicone release compound was applied to one surface of the mold (i.e. on one half), upon which a very thin layer of Silastic® E RTV Silicone Rubber was poured to a thickness roughly half that of the final cast. When cured, 1/4 inch wire mesh was cut and conformed to this half cast surface.

A second layer of silicone rubber was then applied over the screening, a vapor of silicone release compound applied to the other half-mold surface, and both halves of the mold put together.

When this second application had cured, the rubber cast was removed, stiffened by the embedded wire. Except for areas too thin to incorporate the wire screening (e.g. orbital bone), this cast is deformable, keeping the desired shape.

Craniofacial landmarks

The architectural principles employed, as briefly

mentioned above, are fully described in Bromage.²⁴ Their application to KNM-ER 1470 here concerns only the hafting of the facial skeleton onto the calvaria, which was performed on the acquired 3D virtual models. No additional attempts were made here to refine the reconstruction further.

Cephalometric points, planes, and axes (Fig. 3) were defined on right-side *norma lateralis* 3D virtual models of KNM-ER 1470 in the Neutral Horizontal axis (definition below). The decision was made to define architectural relations on the right side because this side better represents the landmarks used in this study. However, this is not a trivial decision because there is downward and forward plastic deformation of the right side affecting the position of P and EAM.^{35,36}

Because of the asymmetry this causes anteriorly, hafting of the face on the calvaria is a compromise of ones own making, particularly in respect to continuity between orbital fragments laterally. There may also be other minor distortions, such as relating to orbital integrity, that would affect our results, but no effort has been made to address them at this time. It must also be noted that landmarks described by Bromage²⁴ pertained to radiographic assessments, which in cases, are slightly different than those definitions arising from their characterization on the cast of KNM-ER 1470 and that are described here:

Orbital midpoint (OM) is observed as the midpoint between preserved right superior and inferior orbital rims.

Orbital Apex (OA) was defined as the midpoint between superior and inferior rims of the right optic canal.

Neutral Horizontal Axis (NHA) is formed as a line connecting OA to OM.

Middle-Anterior Cranial Fossae (MACF) is the junction between the middle and anterior cranial fossae, which is defined as the anterior-most extent of the middle cranial fossa. This region is better preserved on the right size, though it is obscured by several millimeters of matrix at the temporal pole. A point corresponding to MACF was located on the external cranial surface, which was identified.

Maxillary Tuberosity (MT) is defined as the posterior-

inferior point on the maxillary tuberosity behind the last tooth to erupt. However, MT is absent on KNM-ER 1470, the jaw being represented only as far posteriorly as the left mesial M1 alveolus, thus requiring an estimate of MT position to be made (*eMT*). The posterior location of *eMT* was reconstructed by both a comparative statistical approach and a dental surrogate method.

Statistical Estimate of *eMT*. First, covariation between primate maxillary arch length and palatal width was calculated on 300 individuals representing 37 species of extant anthropoids examined by McMahon³⁷ (Table 1).

Palatal width on the comparative primate sample was measured as the inter P3 distance taken at the mesial alveoli. Wood⁶ gives a value of 39mm between the alveoli at P3 midpoints, not at the mesial border, which matched our measurement on the cast. A measure on the cast of the inter P3 distance at mesial borders gives a value of 37mm, there being only a small uncertainty because of some chipping of the left alveolus.

To correct for a contribution of body size to the prediction of palatal width, two proxies available on KNM-ER 1470, were used: glabella-opisthocranion and biporionic breadth (Table 1).

Surrogate Estimate of *eMT*. Independent assessment of *eMT* position was made by reconstructing maxillary arch length with teeth available for other putatively comparable early *Homo* premolars and molars, thus helping to define its posterior position (Table 1). For this, images of KNM-ER 807A, 1590, and 1805 teeth were evaluated for placement in anatomical position, to be situated onto a plasticine reconstruction of the maxillary alveolus (Fig. 6), thus helping to define the anteroposterior position of *eMT*.

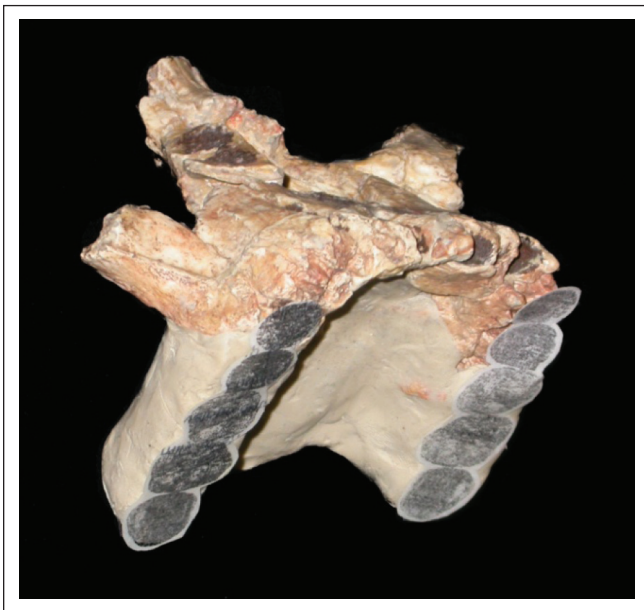


Figure 6. KNM-ER 1470 premolars and molars are represented by KNM-ER 1590 & 806a specimens, permitting *eMT* position to be estimated in the arch posteriorly.

Posterior Maxillary plane (PM) passes between MACF and MT (*eMT*).

Porion (PO) is the midpoint on the upper rim of the External Auditory Meatus.

External Auditory Meatus (EAM) on the right side of KNM-ER 1470 was estimated inferior to PO and between the preserved anterior- and posteriormost limits of the meatus rim.

Posterior Maxillary plane - Neutral Horizontal Axis (PM-NHA) forms the **Posterior Facial Angle (PFA)** between OM-MACF-MT (*eMT*). This angle encloses the facial pocket.

Posterior Facial Angle (PFA) is formed between OM-MACF-MT (*eMT*).

Meatus Angle (MA) is formed between OM-EAM-MT (*eMT*).

Inferior Brain-to-Maxilla Plane (IBMP) is a plane swung posteriorly from its anchoring at MT (*eMT*) and making its first contact with the posterior cranial fossa. The contact point on the posterior cranial fossa is referred to as **Inferior Brain (IB)**.

Prosthion (PR) is defined as the most anterior point on the maxillary alveolar bone between the central incisors.

Alveolon (AN) is defined as the midpoint on the hard palate of a line projected between the maxillary tuberosities.

Maxillary Arch Length (MAL) is the distance between PR and AN.

Anterior Maxillary Hypoplasia (AMH) is the vertical height difference between IBMP projected anteriorly and PR, taken parallel to the PM plane.

Alveolare (AR) is defined as the maxillary alveolar bone apex between the central incisors.

Nasion (N) is the intersection between the internasal and frontonasal sutures, which is observed by Wood⁶ to be 8mm inferior to glabella on KNM-ER 1470.

Facial hafting

The presumptive contact between the facial skeleton and the calvaria was virtually situated on the laser scan image. The facial skeleton was then swung anteroposteriorly until *eMT* touched the PM plane (Fig. 3); the optical topograph was virtually matched to the laser scan (Fig. 4).

This established conditions necessary to satisfy the constrained 90° architectural relationship between the PM plane and NHA.^{22,24}

Cranial capacity estimate

The relationship between prognathism and cranial capacity (CC) for fossil hominin and modern human and chimpanzee crania was examined by Thackeray and Monteith³⁰ and is described by the formula [1]:

$$\log CC = -0.779 \times \log (RPI + 30) + 3.995 [1]$$

where RPI is the Relative Prognathism Index [2], calculated as:

$$RPI = XN/NP \times 100 [2]$$

where X is the point at which a line perpendicular to PO-N, projected beyond N, joins alveolare (A) (Fig. 3).

RESULTS

Craniofacial rendering

Virtual 3D models of KNM-ER 1470 acquired by optical topometry and laser scanning technologies, each acquired from separate 3-part casts, are illustrated in Figures 3 and 4 respectively. PLY format files from each scan were virtually compared and, using the IMInspect module of Polyworks® (InnovMetric Software Inc.), a map of distances between data points (errormap) was color coded. The preponderance of deviations are within 1mm (coded in dark-medium shades of green). This validates for us that architectural relations can be derived independent of the method for acquiring a

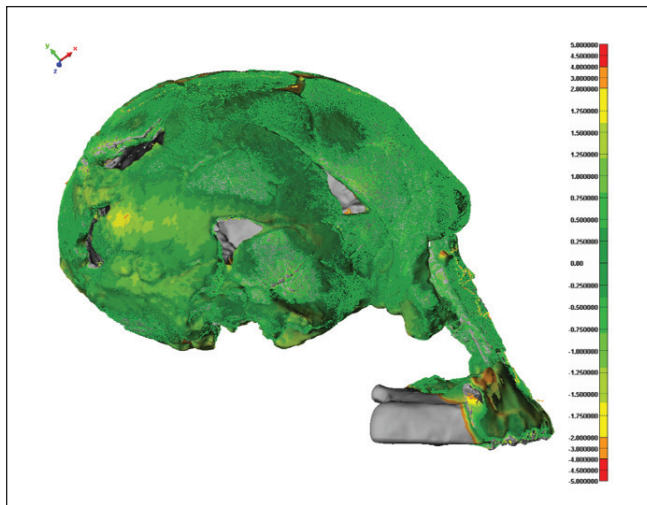


Figure 7. Error-map of the automated virtual alignment comparison between the architecturally constrained optical topometric and laser scanned models of KNM-ER 1470; grey regions are areas of no registration (e.g. the alveolar reconstruction was included in the laser scan only), while good surface matching registration is represented by increasing density of green. Scale bar shows distances and color code relationships.

virtual model (Fig. 7). Visualization of the overlap between models indicates that the scaling and fit are quite satisfactory. Original virtual 3D PLY format files are available upon request.

The flexible cast of KNM-ER 1470 was satisfactorily deformable; we were able to correct some distortion that is apparent in the original non-deformable cast (Fig. 5). We applied nomeasurement protocol for confirming this, however, this being a subjective determination.

Nevertheless, the cast proved convenient for assessing the cranial capacity estimate (see below; Fig. 5).

Craniofacial landmarks

Landmarks, axes, and planes as described in the Materials and Methods were applied to the *norma lateralis* 2D projection of KNM-ER 1470 with Adobe Photoshop CS2 (San Jose, CA) (Fig. 3).

Results of the comparative statistical estimate of KNM-ER 1470 eMT are given in Table 1. Nine different predictor models were examined, using different combinations of sub-groups and predictor variables. For example, Model 1 is with the entire Higher Primate sample of 300 individuals, which includes the body size proxy Neurocranial length; glabella to opisthocranium (NCLGTH) and the cranial predictor Inter-P3 palatal width (P3PALW). Based on this model and measured values for NCLGTH (166) and P3PALW (37), the predicted MXARCL (maxillary arch length; prosthion to alveolon) for KNM-ER 1470 is 77.9 mm, with 95% prediction intervals (similar to confidence intervals, but specific to predicted values) of 89.5 to 66.4 mm.

The first 6 models are for different combinations of sub-groups (Anthropoids, Catarrhines, or Hominoidea) each with one of two different body size proxies: NCLGTH or BIPORB (Biporionic breadth). Models 7-9, do not include a body size proxy in the model. All models include the same cranial predictor, P3PALW.

If we examine the predicted MXARCL and 95% prediction intervals, it is seen that using NCLGTH as the body size proxy has almost no effect on the final predictions: e.g. com-

Table 1. Statistical estimates of KNM-ER 1470 maxillary arch length and eMT position based on nine prediction models and observed KNM-ER 1470 cranial measures (mm): P3PALW, 37; BIPORB, 127; NCLGTH, 166.

Model	Sample	N	Model parameters and estimates								Prediction estimates for KNM-ER 1470 maxillary arch length (MXARCL)		
			Model R-sq	Int Est	Int SE	Body Size	BSP Ext	BSP SE	CP Est	CP SE	MXARCL Est	MXARCL UPL	MXARCL LPL
1	Anthroidea	300	0.86	2.14	0.97	NCLGTH	0.01	0.02	2.00	0.10	77.91	89.47	66.37
2	Anthroidea	300	0.89	1.74	0.84	BIPORB	0.44	0.05	0.73	0.15	84.98	95.42	74.53
3	Catarrhini	183	0.77	7.87	1.70	NCLGTH	0.01	0.03	1.78	0.14	75.61	89.07	62.14
4	Catarrhini	183	0.80	5.96	1.57	BIPORB	0.40	0.06	0.69	0.20	82.31	94.81	69.81
5	Hominoidea	46	0.61	17.06	6.34	NCLGTH	-0.03	0.04	1.66	0.21	72.59	91.00	54.17
6	Hominoidea	46	0.71	3.32	5.87	BIPORB	0.43	0.11	0.61	0.29	80.92	97.43	64.40
7	Anthroidea	300	0.86	2.23	0.93	None			2.04	0.04	77.78	89.28	66.28
8	Catarrhini	183	0.77	7.96	1.68	None			1.82	0.07	75.44	88.84	62.04
9	Hominoidea	46	0.61	15.03	5.84	None			1.57	0.18	73.18	91.43	54.93

Key: Int – intercept; Est – model coefficient estimate; SE – standard error; BSP – body size proxy; CP – cranial predictor, P3PALW was used in all models; UPI – 95% upper prediction limit; LPI – 95% lower prediction limit

pare predictions of Model 1 with Model 7, the two models are the same except for the inclusion of NCLGTH in Model 1, which both give nearly identical MXARCL predictions; the same is true with Model 3 and Model 8, and Model 5 and Model 9. However, using BIPORB in the model does alter the prediction, and they are generally higher.

The model R-square (Model Rsq) values are higher when BIPORB is included, meaning that including BIPORB generally explains more of the variation in MXARCL compared to models with NCLGTH or no body size proxy (this is reflected in the slightly smaller 95% prediction intervals for models with BIPORB: e.g. compare the UPL to LPL range in Model 1 with Model 2.). This means that variance around the prediction line in models with BIPORB are a little tighter than models without it, but the slope is different as well, which accounts for the higher predicted values using BIPORB in the model.

We would like to predict the KNM-ER 1470 MXARCL based on Hominoid data only. Admittedly, there is much variation in the relationship between MXARCL and P3PALW (with or without a body size variable in the model) and the sample size is small, such that prediction intervals for the predicted values are very large if we just include Hominoids. For example, in Model 9, (Hominoids, n=46, with no body size proxy, only predicting MXARCL from P3PALW) the predicted value of the KNM-ER 1470 MXARCL is 73.18 but the 95% prediction limits are 91.4 to 54.9. If you use the entire Anthropoid sample (n=300) as in Model 7, the predicted value of the KNM-ER 1470 MXARCL is 77.78 and the 95% prediction limits are 89.28 to 66.28.

Despite this substantial variation in the estimated MXARCL values predicted by the models, as we will see below, all of the predicted values indicate a more prognathic facial orientation for KNM-ER 1470.

For the surrogate estimate of KNM-ER 1470 eMT we observe that the average postcanine tooth row length, between the most minimum and maximum length assemblies of P3-M3 mesiodistal diameters, is 61.2mm (Table 2). This happens also to be the value represented by the KNM-ER 1590 left P3-M2 plus KNM-ER 807A right M3, allowing the most teeth to be represented by the fewest surrogate individuals. These teeth were situated in anatomical position

Table 2. Mesiodistal Diameters (mm x 10; corrected) from Wood ⁶

Tooth Type	KNM-ER 807A	KNM-ER 1590	KNM-ER 1805B
P3		104 (L); 106 (R)	
P4		107 (L); 107 (R)	
M1		141 (L); 142 (R)	132 (R)
M2		146 (L)	128 (L); 133 (R)
M3	114 (R)		136 (L); 138 (R)

(transverse plane only), rendering a 60mm P3-M3 dental arch anteroposteriorly, which was superimposed onto a maxillary arch formed in modeling clay for determining the position of eMT (Fig. 6).

Measurement of KNM-ER 1470 maxillary arch length, PR to AN, using the surrogate method gives a value of 73mm to a line projected between left and right eMTs. This value is veritably identical to the value obtained using Hominoids in the statistical evaluation (large prediction limits notwithstanding). While this measurement is conservative relative to other statistical models, it was used to position eMT.

MA is arbitrarily illustrated on a virtual model of KNM-ER 1470 with 45° and situated so that its superior line segment passes from its origin at EAM to intersect OM (Fig. 3). The inferior line segment does not intersect eMT, but, rather, lays superior to it. For comparison, an inferior line segment intersecting eMT is also illustrated, which results in an MA of 60°.

Facial hafting

The KNM-ER 1470 calvaria is aligned with NHA in the horizontal, which is the effective neutral head position in life (Fig. 3-4). Positioning of the facial skeleton onto the calvaria was established by anterior-posterior virtual rotation of the facial part at its articulation around N such that eMT position lay on the PM plane when PM-NHA equals 90°. This occurs when the right PO-PR distance equals 145mm, or right PO-AR distance equals 147mm.

The IB, MT, and PR are on or close to the same plane (IBMP) for most mammals. However, as noted for anthropoids by Enlow and Azuma ²², KNM-ER 1470 exhibits a vertical hypoplasia of the anterior maxilla so that PR is positioned above IBMP (Fig. 3).

Cranial capacity estimate

The corrected craniofacial architecture of KNM-ER 1470 provides the opportunity to evaluate the cranial capacity estimate of 752cc²⁹. The formula [1] (see Methods) describing the relationship between prognathism and cranial capacity³⁰ results in the following: normalized measures of XN (4.62) and NP (95.38), which result in a Relative Prognathism Index (RPI) [2] of 4.84, the outcome of which is a log CC of 2.795. This corresponds to a cranial capacity of 625 cc (1 SD = 49cc). An RPI of 4.84 is greater than the RPI of 2.7 originally posited for KNM-ER 1470 by Thackeray and Monteith.³⁰ This is because they used the original cranial capacity estimate of 752cc to back-reconstruct RPI. The RPI by our research, now being better constrained architecturally, indicates that the cranial capacity may be reduced from the original estimate.

DISCUSSION

Biological principles governing craniofacial architecture were incompletely known when KNM-ER 1470 was discovered, thus the relative orthognathy and cranial capacity posited for this specimen were free to satisfy our collective preconception of the shift from more ape-like relationships and proportions, such as represented by the genus *Australopithecus*, to those that were more human-like. It was as if to be *Homo* it should have a large brain and a vertical face. A

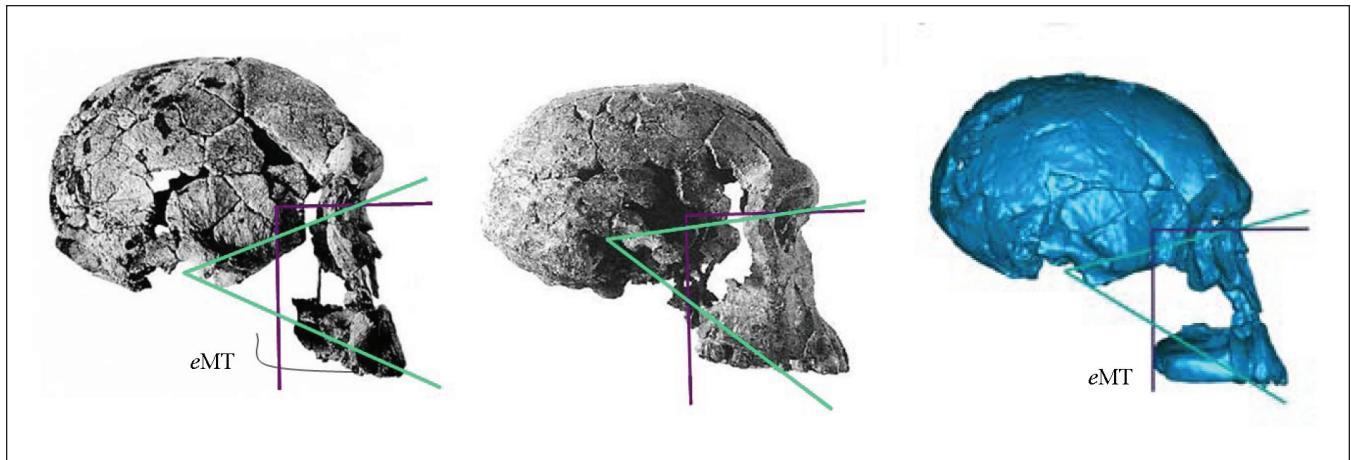


Figure 8. The PFA and MA are illustrated on KNM-ER 1470 (left) and on the relatively intact calvaria of KNM-ER 1813 (middle).⁸ For comparison, the architecturally constrained reconstruction is shown at right.

reconstruction of KNM-ER 1470 according to mammalian architectural constraints outlined by Enlow and Azuma²² demonstrates that this early *Homo* specimen is, by comparison to our common appreciation, relatively prognathic.

If we compare the relatively more intact early *Homo* skull, KNM-ER 1813, and that of KNM-ER 1470, discrepancies are revealed in architectural relationships (Fig. 8). The inferior line segments of 45° MAs are short of intersecting MT and eMT on both specimens respectively, recounting the architectural inconsistency of MA noted by Bromage.²⁴ However, while the inviolate association between MT and the PM Plane is correct on KNM-ER 1813 and posing no architectural conundrum, the originally assembled KNM-ER 1470 reveals a PM Plane descending anterior to an intersection with eMT, indicating a relatively orthognathic facial skeleton inconsistent with architectural constraints governing mammalian craniofacial anatomy.

For KNM-ER 1470 to be as orthognathic and still conform to the MT-PM constraint, the specimen's maxillary arch length would have to be much shorter than indicated by both comparative analyses and surrogate reconstruction.

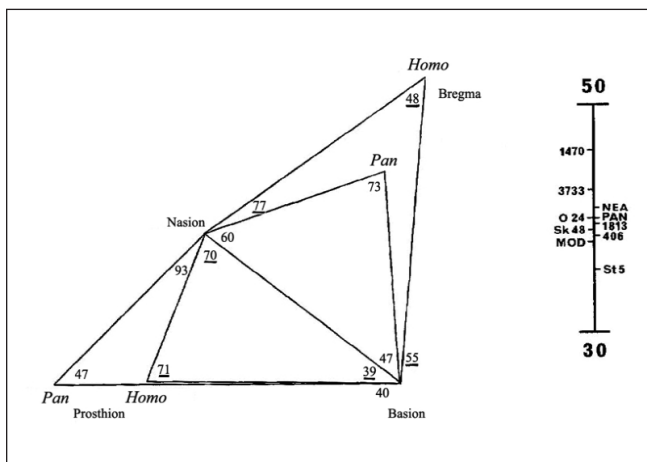


Figure 9. Mean craniofacial angle values for *Pan* and *Homo* (left). Note the high KNM-ER 1470 Nasion-Basion-Prosthion angle as compared to other Plio-Pleistocene hominids (right; MOD refers to modern *Homo*). Modified from Stringer 39 (his Figures 2-3).

Establishing eMT and PFA conformation to the mammalian architectural constraint is a first step in reconstructing the KNM-ER 1470 craniofacial skeleton, a strategy also taken in the reconstruction of the substantially distorted 7 m.y. hominid calvaria, *Sahelanthropus tchadensis*, from Chad.³⁸

Architectural discrepancy is suggested in published assessments of KNM-ER 1470. For instance, Stringer³⁹ estimated *Pan*-like (prognathic) values for the prosthion and nasion angles, but an unusually high value for the basion angle compared with both *Pan* and *Homo*, based on estimated length measures from casts of basion-prosthion (124mm), basion-nasion (95mm), and nasion-prosthion (89.5mm) (Fig. 9 right). However, Stringer recalls that this facial configuration was a compromise between Alan Walker's preliminary reconstruction and another by Bernard Denston of the Duckworth Laboratory, Department of Biological Anthropology, University of Cambridge, believed to be relatively prognathic compared to the provisionally assembled original illustrated by Leakey¹ (Stringer, pers. comm.).

Thus compared to the original KNM-ER 1470 assembly illustrated in Leakey,¹ relatively prognathic reconstructions do exist, some possibly resembling the architecturally constrained rendering illustrated here. Alan Walker's unpublished preliminary reconstruction, presently available as a one-part cast for purchase from Kenya National Museum, is rather prognathic, though Stringer's work (above) suggests that it may be orthognathic in comparison to our architecturally constrained reconstruction. In order to visualize a possible difference between reconstructions, we obtained a laser scanning 3D PLY format file acquired from a Kenya National Museum one-part cast (courtesy of Philip Gunz, Max Plank Institute) for comparison of virtual models.

A bestfit routine for comparing virtual models of the one-part and architecturally constrained reconstructions was performed as before, but we first ignored data from the facial region of the latter. Then we restored facial data from our architecturally constrained reconstruction, once again using the IMinspect module of Polyworks, to produce a color

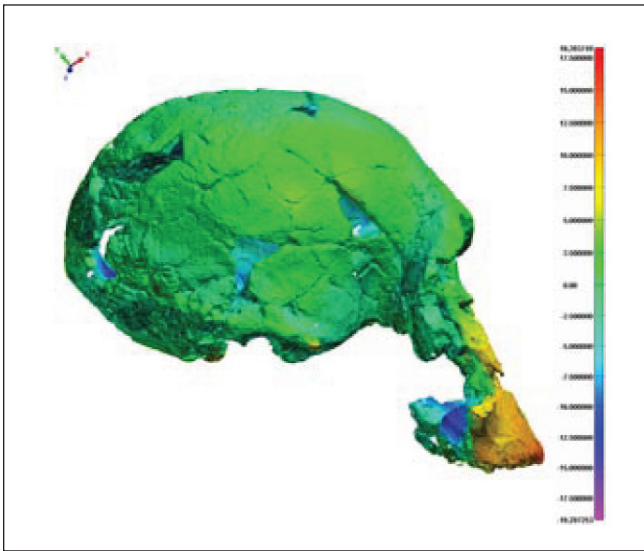


Figure 10. Error-map of the automated virtual alignment comparison between the architecturally constrained optical topometry model (visible) and the Kenya National Museum one-part laser scanned model (hidden) of KNM ER 1470. Good surface registration is represented by shades of green, while shades of orange and red indicate prognathism of the architecturally constrained model. Scale bar shows distances and color code relationships. (Note that the blue color shows negative distance, which is probably the case for some data derived from the facial part of the three-part cast. This is because of missing details in the one-part-reconstruction. There is also a problem encountered in the bestfit comparison of internal surface structures; the one-part reconstruction does not possess valuable internal surface information due to addition of artificial materials).

coded error map on the architecturally constrained reconstructions, while hiding the one-part rendering data (Fig. 10).

Data from the calvaria match in a bestfit model very well (shades of green). However, the architecturally constrained reconstruction is more prognathic in shades of orange and red; at the nasal region we have relatively little difference, but at PR it is approximately 18mm.²⁸

Another preliminary reconstruction by Alan Walker was used by Jay Matternes for fleshing out the physiognomy of early *Homo*.⁴⁰ This reconstruction was relatively prognathic, as far as one can discern from the oblique views illustrated, and it is reasonable to assume that Richard Leakey and consulted colleagues sanctioned this perspective.

Nevertheless, irrespective of the degree to which various reconstructions were more or less prognathic, we have presented here a biological appreciation for the construction of the mammalian skull and some of the tools that enable an architecturally constrained hafting of the facial skeleton to the calvaria when the association is uncertain, as it is for KNM-ER 1470.

Anyone with a three-part cast of KNM-ER 1470 can easily reconstruct the skull by articulating the facial skeleton at N and rotating the maxilla forward until the PO-AR distance is 147mm on the right side. This represents a small increase over the right PO-AR distance of 137mm previously estimated by Wood.⁶

The relationship between facial prognathism and brain

size is also an important finding of craniofacial architectural research. We are reminded that the reference planes and angles investigated by Enlow and Azuma²² explicitly characterized craniofacial relations between the brain and facial growth vectors that determine the size and disposition of the mammalian facial complex and space available for the airway and esophagus. The PM Plane, or boundary, described by Enlow and Azuma,²² is a natural anatomical interface between the neurocranium and the face, structurally linked at 90° to the NHA, which establishes the facial growth vector. This relationship is maintained throughout growth and is developmentally constrained among mammals in general.

Two scale-related quantities that can potentially affect nasomaxillary morphology and spatial position are the shape and relative size of the brain. Consistent with the hypotheses of Dabelow,⁴¹ Biegert,⁴² Huxley,⁴³ Weidenreich,⁴⁴ Enlow and McNamara,⁴⁵ and Enlow,⁴⁶ the effects of relative brain size on nasomaxillary morphology are mediated indirectly through changes to the chondrocranium.³⁷ A best fit covariance structural model confirmed the hypothesis of Enlow and McNamara⁴⁵ that cribriform plate orientation is the primary mediator between the development and evolution of the brain and nasomaxillary morphology.³⁷ Multi-level and ontogenetic analysis further indicated that changes in relative brain size and concomitant changes in cribriform plate orientation affect changes to nasomaxillary form through both acclimative and selective nomological processes. These results are consistent with current morphogenetic theory, which indicates that all three types of cellular control stimuli (intrinsic genetic, epigenetic and environmental) act to regulate morphogenesis of the viscerocranium and skeletogenesis of the chondrocranium.

A proposed invariant 90° angle beside that of the PFA, between the cribriform plate and midfacial plane⁴⁵ that translates changes in brain form to changes in facial growth vectors, has also been confirmed for anthropoids.³⁷ That this angle is biologically constrained was demonstrated using a regression-based test for angular invariance (Appendix A). It was shown that although changes in basicranial angle can affect the orientation of the cribriform plate (especially in catarrhines), the latter has a strong and independent influence on nasomaxillary morphology. Covariance structural analysis indicated that cribriform plate orientation mainly effects changes in the nasomaxillary skeleton by influencing the degree of facial prognathism during development.³⁷ Disagreement between investigators about the existence of primate cribriform plate-midfacial plane constraint in particular, and thus the identification of biological constraint in general, has motivated us to provide statistical support and discussion in Appendix B, derived from reference 37.

We believe that an explanation for the relationship between facial prognathism and brain size relates to stability of the center of mass of the craniofacial complex during locomotory behavior.⁴⁷ Stability of craniofacial center of mass during locomotory behavior is essential for navigating, acquiring mobile food resources, evading predators, etc. The

90° angular architectural constraint noted above, between the cribriform plate and midfacial plane, and that between the PM Plane and NHA is thus a profound adaptation. This adaptation constrains the distribution of mass to allow effective proprioceptive feedback control of the neck musculature/ligaments to stabilize line of sight and field of view during locomotory activities.^{cf 48}

The relationship between hominoid and hominid prognathism and brain size we observe provides a rationale for evaluating the KNM-ER 1470 cranial capacity. Thackeray⁴⁹ first queried the cranial capacity, suggesting, on the basis of a known endocast fit to the right calvaria element, that the estimate should be reduced. We found that a 675cc deformable volume (near 1SD above the 625cc estimate) satisfactorily impressed into cranial fossae of the flexible cast (Fig. 5), this being also a practical demonstration of the effect of what a seemingly minor rotation of left and right calvaria parts against their sagittal contact can have on the estimated cranial capacity.

Another 25cc is considered by us able to penetrate into an aggregate of other small interstices, thus we feel that a ca. 700cc estimate may be realistic. This revision is not inconsistent with other Late Pliocene *Homo* prior to the appearance of Early Pleistocene *Homo erectus/ergaster*.⁵⁰ KNM-ER 1470, now regarded as representing *Homo rudolfensis*, which is the earliest recognized representative of the genus *Homo*, might now be considered to be partly defined on the basis of its relative prognathism and somewhat smaller brain size.

The revised reconstruction also confirms (and increases) the previously described MA of KNM-ER 1470,²⁴ demonstrating the somewhat unsatisfactory utility of MA for demonstrating architectural principles. However, should there be any significance to the high MA values for KNM-ER 1470, KNM-ER 1813, and other Plio-Pleistocene hominids, then it is to unite *Paranthropus* and early *Homo* morphotypes. A persistent theme in paleoanthropology has been the identification of many morphological⁵¹⁻⁵⁸ and ontogenetic⁵⁹ similarities between *Paranthropus* and *Homo*, most of which are interpreted as homoplasies. A shortcoming of the reconstruction presented here is that, beyond the heuristic usefulness of the deformable cast (Fig. 5), we have not considered the plastic deformation observed on KNM-ER 1470.³⁶ This will have some effect on the position of PR and on MA particularly, the consequences diminishing anteriorly. If MACF was displaced significantly anteriorly, this would have an effect on the anteroposterior location of eMT, artificially increasing the degree of prognathism and diminishing the cranial capacity estimate even more according to the methods described here. We believe the likelihood of this is small, but agree that it will be useful to perform a more sophisticated virtual reconstruction, which may morph the KNM-ER 1470 model to reduce or eliminate the distortion. An alternative would have been to base the architectural diagnostics on the left, but we elected not to do this for reasons of having less well preserved landmarks on that side.

That we have performed our reconstruction using a cast

should be explicit. Small measurement variations will exist between casts of KNM-ER 1470. Casting materials typically shrink by some small percentage during curing, and it may even be that seasonal variations in humidity, together with minor changes in casting material properties over the decades, is responsible for some of this variation. However, in our study, characterized in all by angular relationships and proportions except for palatal width (which in our cast matched the published value), we are not apt to be significantly affected by such variations. Nevertheless, computed tomography of the KNM-ER 1470 original will be helpful for improving results based on the analytical approach taken here. It is also and obviously *not* wonderful that our analysis depends upon the reconstruction of a landmark that does not exist on KNM-ER 1470. While this only engenders uncertainty, we are at least a little satisfied that two completely independent methods provided an estimate of the position of MT that was virtually identical.

Lastly, we should point out that the database used by Thackeray and Monteith³⁰ concerning the relationship between prognathism and brain size was not homogenous. These authors were looking for a pattern in an exploratory study, hoping to quantify a relationship that applied to hominoids in general. They noted an inverse relationship between RPI and cranial capacity (the pattern), and they attempted to quantify it using least squares regression analysis. However, the possibility exists that the ape and human sample may cluster by phylogeny, and thus conventional regression may be inappropriate. The sample size of ape and human crania used by Thackeray and Monteith³⁰ is considered to be rather small for performing a phylogenetic Generalized Least Squares analysis, but one should be performed on a larger sample in order to examine the possibility of bias and to correct for this.⁶⁰ Having said this however, it is of interest to note that McMahon³⁷ also found a highly significant inverse relationship between prognathism and endocranial volume in subgroups of anthropoids, cararrhines, and hominoids, when controlling for phylogenetic clustering. Appendix C provides the statistical results of this relationship.

While these methodological and sampling difficulties, if resolved, would alter in some respects the results of this study, we at least believe that the prognathism as reconstructed here is a closer approximation to the original conformation in life and, as such, so too the cranial capacity estimate. The values of both prognathism and cranial capacity need not be taken as final, but more true to the original condition in life we believe them to be.

CONCLUSIONS

Based upon our preconceptions of what craniofacial traits to expect in a Plio-Pleistocene representative of the genus *Homo*, the KNM-ER 1470 skull was originally assembled with a relatively large brain and vertically oriented face. However, to be consistent with mammalian architectural relationships, the face must have been relatively prognathic. Furthermore, the relationship between facial prognathism and brain size, which is hypothesized to relate to head pos-

ture during locomotor activity, suggests a small downward estimate of the cranial capacity.

Biological principles that govern the design of the craniofacial skeleton provide a major contribution to studies of human anatomy, development, and evolution. Following an architecturally constrained reconstruction procedure, the Gestalt perspective of KNM-ER 1470, we conclude, is that of a relatively prognathic skull harboring a cranial capacity of about 700cc.

In this research we became more than usually aware of the tendency we have (as humans) for limiting our perceptions of morphology as a result of preconceived notions. While no simple matter to address, attention to this behavior is critical to the performance of relatively unbiased research. In an effort to reveal and address our own bias (i.e. the authors of this article), we attempted a novel review procedure, which was at least partly successful (cf. Acknowledgments). Of course, a major tenet of science is perceived objectivity, but in practice this has complexity written all over it. "The problem a scientist or engineer chooses to solve and the way he breaks that problem or system down into components is a choice of his making; it is a function of among other things, his particular scientific technical training and his personality. In short, what one observes is a basic function of what one has been trained to observe."⁶¹

The original KNM-ER 1470 as originally assembled was entirely consistent and valid within the psychosocial realm that generated it. Though we remain cognizant of the difficulty of addressing our preconceptions, it would be well to recognize in ourselves the interdependence between observer and the phenomena investigated, as aptly stated by Mitroff⁶¹ above. Ample research in perceptual learning makes clear that our perceptions of the world are unconsciously modified by experience.⁶² The strategy the brain uses depends upon this experience, readily "seeing" objects according to representations in the cortical sensory pathway that build with each inculcation. This can hardly have been more potently stated by Kosslyn *et al.*⁶³; "knowledge can fundamentally bias what one sees". An additional component to consider is our capacity through attention to select all attributes of an object as a whole, these attributes being linked by Gestalt rules.⁶⁴ We feel that paleoanthropology has been particularly given to the combination of perceptual bias and its associated Gestalt rules from which major paradigms based on interpretations of morphology are formed. The reconstruction of KNM-ER 1470 presented here is an attempt to constrain our bias and modify the Gestalt perspective, albeit one with a view to empirical support that was heretofore unavailable.

ACKNOWLEDGEMENTS

Versions of this paper have been previously reported at *African Genesis: A symposium on hominid evolution in Africa*, Johannesburg, January 8-14, 2006, and to joint meetings of the *International, American, and Canadian Associations of Dental Research*, New Orleans, March 21-24, 2007. We thank Astrid Bender and Sebastian Lüpfer for

constructing the flexible cast of KNM-ER 1470, the NYCEP Morphometrics Group (E. Delson, W. Harcourt-Smith) and Anthony Pagano for assistance with laser scanning of the KNM-ER 1470 cast. Thanks also to Chris Stringer, British Museum of Natural History, for information concerning his 1986 study of KNM-ER 1470, and to Philip Gunz, Max Planck Institute for Evolutionary Anthropology, for the laser scan 3D PLY file of the Kenya National Museum's one-part cast of KNM-ER 1470. Support for this work was generously provided by the Faculty and Staff Development Council of the New York University College of Dentistry. An earlier draft of this paper was widely distributed according to an open peer-review protocol outlined in Bromage.⁶⁵ We are particularly grateful to Alan Walker for his comments.

APPENDICES

Due to the limitation in space in the journal, the complete manuscript with appendices can be seen online or may be obtained directly from the corresponding author.

REFERENCES

1. Leakey R.E.F. Evidence for an advanced Plio-Pleistocene hominid from East Rudolf, Kenya. *Nature*, 242: 447-450, 1973.
2. Day M.H., Leakey R.E.F., Walker A.C. and Wood B.A. New hominids from East Rudolf, Kenya, I. *Am J phys Anthropol*, 42: 461-476, 1975.
3. Lewin R. *Bones of Contention: Controversies in the Search for Human Origins*. Simon & Shuster Inc., New York; 1987.
4. Reader J. *Missing links: The hunt for earliest man*. Penguin Group, London; 1988.
5. Willis D. *The hominid gang: Behind the scenes in the search for human origins*. Penguin Group, New York; 1989.
6. Wood B. *Koobi Fora research project: Volume 4. Hominid cranial remains*. Oxford University Press, Oxford; 1991.
7. Walker A.C. and Shipman P. *The wisdom of the bones: In search of human origins*. Random House Inc, New York; 1996.
8. Leakey R.E.F. Hominids in Africa. *Am Sci*, 64: 174-178, 1976.
9. McDougall I., Maier R., Sutherland-Hawkes P. and Gleadow A.J.W. K-Ar age estimate for the KBS Tuff, East Turkana, Kenya. *Nature*, 284: 230-234, 1980.
10. McDougall I. 40Ar/39Ar age spectra from the KBS Tuff, Koobi Fora Formation. *Nature*, 294: 120-124, 1981.
11. Bromage T.G. Ontogeny and evolution of primate and early hominid craniofacial architectural constraints. *Am J phys Anthropol*, Suppl 12: 54, 1991.
12. Enlow D.H. A morphogenetic analysis of facial growth. *Am J Orthod*, 52: 283-299, 1966.
13. Thompson D'Arcy W. *On growth and form*. Cambridge University Press, London; 1942.
14. Enlow D.H. *The human face: An account of the postnatal growth and development of the craniofacial skeleton*. Harper and Row, New York; 1968.
15. Enlow D.H., Hunter W.S. The growth of the face in relation to the cranial base. *Eur Orthod Soc Congress Report*, 44: 321-335, 1968.
16. Enlow D.H., Moyers R.E., Hunter W.S. and McNamara Jr.J.A. A procedure for the analysis of intrinsic facial form and growth. *Am J Orthod*, 56: 6-23, 1969.
17. Enlow D.H., Kuroda T. and Lewis A.B. The morphological and morphogenetic basis for craniofacial form and pattern. *Angle Orthod*, 41: 161-188, 1971.
18. Enlow D.H., Kuroda T. and Lewis A.B. Intrinsic craniofacial compensations. *Angle Orthod*, 41: 271-285, 1971.
19. Enlow D.H. and Moyers R.E. Growth and architecture of the face. *J Am Dent Assoc*, 82: 763-774, 1971.

20. Enlow D.H. Croissance et architecture de la face. *Pedod Fr*, 6: 122–144, 1974.
21. Bhat M. and Enlow D.H. Facial variations related to headform type. *Angle Orthod*, 55: 269–280, 1985.
22. Enlow D.H. and Azuma M. Functional growth boundaries in the human and mammalian face. In: Langman J., editor. *Morphogenesis and malformations of the face and brain*. The National Foundation, New York; 217–230, 1975.
23. Bromage T.G. Faces from the past. *New Scientist*, 1803: 38–41, 1992.
24. Bromage T.G. The ontogeny of *Pan troglodytes* craniofacial architectural relationships and implications for early hominids. *J hum Evol*, 23: 235–251, 1992.
25. Ravosa M.J. and Shea B.T. Pattern in craniofacial biology: evidence from the Old World monkeys (Cercopithecidae). *International Journal of Primatology*, 15: 801–821, 1994.
26. Lieberman D.E. Sphenoid shortening and the evolution of modern human cranial shape. *Nature*, 393: 158–162, 1998.
27. Lieberman D.E. and McCarthy R.C. The ontogeny of cranial base angulation in humans and chimpanzees and its implications for reconstructing pharyngeal dimensions. *J hum Evol*, 36: 487–517, 1999.
28. McCarthy R.C. and Lieberman D.E. 2001 Posterior maxillary (PM) plane and anterior cranial architecture in primates. *Anat Rec*, 264: 247–260, 2001.
29. Holloway R.L. Human paleontological evidence relevant to language behavior. *Human Neurobiology*, 2: 105–114, 1983.
30. Thackeray J.F. and Monteith B.D. Relationships between cranial capacity and prognathism in Plio-Pleistocene hominids. *South African J Sci*, 93: 289–291, 1997.
31. Rosenberger A.L. Protoanthropoidea (Primates, Simiiformes): A new primate higher taxon and a solution to the *Rooneyia* problem. *J Mamm Ev*, 13: 139–146, 2006.
32. Rosenberger A.L. and Hogg R.T. On *Bahinia pondaungensis*, an alleged early anthropoid. *Paleoanthropology*, 2007: 26–30, 2007.
33. Kullmer O., Huck M., Engel K., Schrenk F. and Bromage T.G. Hominid Tooth Pattern Database (HOTPAD) derived from Optical 3D Topometry. *British Archeological Reports*, S1049: 71–82, 2002.
34. Dow Corning (2007) Available: <http://www.dowcorning.com/applications/search/default.aspx?R=23EN&DCCSF=260EN> Accessed February 22, 2008.
35. Oyen O.J. and Walker A. Stereometric craniometry. *Am J phys Anthropol*, 46: 177–182, 1977.
36. Walker A.C. The Koobi For a hominids and their bearing on the origins of the genus *Homo*. In: Sigmon B.A. and Cybulski S., editors. *Papers in honor of Davidson Black*. University of Toronto Press, Toronto; 193–215, 1981.
37. McMahon J.M. Dissertation: Nomological mechanisms of anthropoid nasomaxillary diversity. City University of New York, New York; 1999.
38. Zollikofer C.P.E., Ponce de León M.S., Lieberman D.E., Guy F., Pilbeam D., Likius A., Mackaye H.T., Vignaud P. and Brunet M. Virtual cranial reconstruction of *Sahelanthropus tchadensis*. *Nature*, 434: 755–759, 2005.
39. Stringer C.B. The credibility of *Homo habilis*. In: Wood B.A., Martin L. and Andrews P., editors. *Major topics in primate and human evolution*. Cambridge University Press, Cambridge; 266–294, 1986.
40. Leakey R.E.F. Skull 1470. *National Geographic*, June: 818–829, 1973.
41. Dabelow A. Über Korrelationen in der phylogenetischen Entwicklung der Schädelform. I Die Beziehungen zwischen Rumpf und Schädelform. *Morphol Jahrb*, 63: 1–49, 1929.
42. Biegert J. Der formwandel der primaten schadels und seine beziehungen zur ontogenetischen (Entwicklung und den phylogenetischen spezialisationes der kopforgane). *Gegnbrs Morphol Jhb*, 98: 77–199, 1957.
43. Huxley T.H. Evidence as to Man's Place in Nature. Williams and Norgate, London; 1863.
44. Weidenreich F. Generic, specific, and subspecific characters in human evolution. *Am J phys Anthropol*, 31: 413–431, 1947.
45. Enlow D.H. and McNamara J.A. The neurocranial basis for facial form and pattern. *Angle Orthod*, 43: 256–270, 1973.
46. Enlow D.H. *Handbook of facial growth*. WB Saunders, Philadelphia; 1975.
47. Bramble D.M. Head stabilization and locomotor behavior in the Hominidae. *Am J phys Anthropol*, 81: 197–198, 1990.
48. Bramble D.M. and Lieberman D.E. Endurance running and the evolution of *Homo*. *Nature*, 432: 345–352, 2004.
49. Thackeray J.F. Alternative views on hominid diversity in the context of Darwin's assessment of barnacles. In *Towards Gondwana Alive*. Gondwana Alive Society, Pretoria; 106–108, 1999.
50. Holloway R.L. Evolution of the human brain. In: Lock A. and Peters C., editors. *Handbook of human symbolic evolution*. Oxford University Press, New York; 74–116, 1996.
51. Bromage T.G., Schrenk F. and Zonneveld F.W. Palaeoanthropology of the Malawi Rift: An early hominid mandible from the Chiwondo Beds, northern Malawi. *J hum Evol*, 28: 71–108, 1995.
52. Dean M.C. *Homo and Paranthropus*: Similarities in the cranial base and developing dentition. In: Wood B.A., Martin L. and Andrews P., editors. *Major topics in primate and human evolution*. Cambridge University Press, Cambridge; 249–265, 1986.
53. Dean M.C. Growth processes in the cranial base of hominoids and their bearing on morphological similarities that exist in the cranial base of *Homo* and *Paranthropus*. In: Grine F.E., editor. *Evolutionary history of the "robust" australopithecines*. Aldine de Gruyter, New York; 107–112, 1988.
54. Dean M.C. and Wood B.A. Metrical analysis of the basicranium of extant hominoids and *Australopithecus*. *Am J phys Anthropol*, 54: 63–71, 1981.
55. Dean M.C. and Wood B.A. Basicranial anatomy of Plio-Pleistocene hominids from East and South Africa. *Am J phys Anthropol*, 59: 157–174, 1982.
56. Kimbel W.H., White T.D. and Johanson D.C. Cranial morphology of *Australopithecus afarensis*: a comparative study based on a composite reconstruction of the adult skull. *Am J phys Anthropol*, 64: 337–388, 1984.
57. Skelton R.R., McHenry H.M. and Drawhorn G.M. Phylogenetic analysis of early hominids. *Cur Anthropol*, 27: 21–43, 1986.
58. Tobias P.V. Numerous apparently synapomorphic features in *Australopithecus robustus*, *Australopithecus boisei* and *Homo habilis*: Support for the Skelton-McHenry-Drawhorn hypothesis. In: Grine F.E., editor. *Evolutionary history of the "robust" australopithecines*. Aldine de Gruyter, New York; 293–308, 1988.
59. Bromage T.G. Ontogeny of the early hominid face. *J hum Evol*, 18: 751–773, 1989.
60. Spoor F., Garland Jr.T., Krovitz G., Ryan T.M., Silcox M.T., and Walker A. The primate semicircular canal system and locomotion. *Proc Nat Acad Sci* 104: 10808–10812, 2007.
61. Mitroff I.I. Simulating engineering design: Philosophical presuppositions in engineering education and in models of the engineering design process. *Skyscraper Engineer*, 20: 9–33, 1970.
62. Tsodyks M. and Gilbert C. Neural networks and perceptual learning. *Nature*, 431: 775–781, 2004.
63. Kosslyn S.M., Thompson W.S., Kim I.J. and Alpert M. Topographical representations of mental images in primary visual cortex. *Nature*, 378: 496–498, 1995.
64. Blaser E., Pylyshyn Z.W. and Holcombe A.O. Tracking an object through feature space. *Nature*, 408: 196–199, 2000.
65. Bromage T.G. Science networks and the future of integrative research. In: Bromage T.G., Vidal A., Aguirre E. and Perez-Ochoa A., editors. *Integrative Approaches to Human Health and Evolution*. Elsevier, Amsterdam; 160–174, 2006.

Appendix A

Regression of facial prognathism on cribriform plate orientation. Data were adjusted for phylogenetic clustering using phylogenetic autocorrelation. (N = 300; across 37 species of anthropoids.).

Partial regression of facial prognathism on cranial base angle and cribriform plate orientation		
Taxon	Maximum likelihood regression coefficients (95% CI, and p-values) of facial prognathism on cranial base angle controlling for cribriform plate orientation	ML partial regression coefficients (95% CI, and p-values) of facial prognathism on cribriform plate orientation controlling for cranial base angle
Anthropoids (n=300)	0.24 (0.16, 0.32) p = .0001	0.31 (0.24, 0.38) p = .0001
Platyrrhini (n=117)	0.14 (-0.02, 0.30) p = .08	0.30 (0.22, 0.38) p = .0001
Atelidae (n=65)	0.36 (0.08, 0.64) p = .01	0.39 (0.28, 0.49) p = .0001
Cebidae (n=52)	0.07 (-0.09, 0.24) p = .37	0.14 (0.04, 0.24) p = .004
Catarrhini (n=183)	0.23 (0.15, 0.32) p = .0001	0.45 (0.34, 0.57) p = .0001
Cercopithecoidea (n=137)	0.07 (-0.04, 0.19) p = .22	0.32 (0.19, 0.44) p = .0001
Cercopithecinae (n=87)	-0.06 (-0.20, 0.07) p = .36	0.29 (0.15, 0.44) p = .0001
Colobinae (n=50)	0.45 (0.21, 0.69) p = .0001	0.18 (-0.03, 0.39) p = .09
Hominoidea (n=46)	0.20 (0.04, 0.37) p = .01	0.67 (0.44, 0.91) p = .0001

Appendix B

The question of how much variation is ‘acceptable’ in order to recognize the existence of a biological constraint has yet to be adequately addressed. Ravosa and Shea¹ devised four criteria for assessing angular invariance. These included: (1) no significant correlation between the proposed invariant angle and size, (2) no significant differences between the angular means of various subtaxa, (3) a low angular standard deviation compared to other angles, and (4) a low angular coefficient of variation (CV) compared to other angles. We can readily dismiss three of the four criteria. The notion that character invariance resulting from a morphogenetic constraint on form should not be correlated with size holds no theoretical or analytical credibility. Such non-random variation is expected if interactive effects are in operation. Ravosa and Shea¹ have conflated invariance with independence, and isometry due to scaling effects with geometric invariance due to constraint. By adhering to a strict criterion of invariance that is independent of covariate interaction effects (i.e., taxa or size, and one could also include sex, age, habitat, etc.), these authors provide an untenable model for the identification of biological constraints, a model that contains no provisions for examining how a given constraint behaves under varying genetic, epigenetic and environmental conditions.

Aside from these substantive theoretical objections, there are, in addition, several analytical problems with their choice of analyses. Since the correlation coefficient is partly determined by the variance of the variables under study it cannot be used as an independent test of the degree of variability exhibited by a character. Likewise, ANOVA tests for mean differences among taxa are invalid tests of invariance because they are variance standardized. In an ANOVA the among-groups variance is assessed in relation to the total (pooled within-groups) variance, and therefore, variables with high total variance are no more or less likely to exhibit

significant mean differences among taxa than variables with low total variance. More informative would have been Cochran's C or the Bartlett-Box test for homogeneity of variance. Use of the coefficient of variation (CV) with angular measures is a more obvious transgression of morphological analysis. The CV was designed as a measure of variability that takes into account the size of the structures being measured². It is valid only when applied to size-dependent variables such as linear distances, and it is invalid when applied to angles and other shape variables that are size-independent. Simpson and colleagues³ aptly expressed this principle as follows: "The valid use of V [coefficient of variation] depends on the assumption that variation as a biological function is relative to absolute size or, in terms of distributions, that absolute dispersion increases in direct proportion to the mean [size]" (p. 90). Since the variances of angular measures are not expected to covary with their means, "...use of the coefficient of variability in comparisons involving the variability of morphological relationships [such as 'angular relationships'] can lead to completely erroneous conclusions"⁴ (p. 248).

Measures of dispersion (such as the standard deviation) remain the only valid measures of variability for angular data. But how is one to determine the level of variability that is acceptably low enough to indicate the operation of a biological constraint? Ravosa and Shea¹ (p. 808), who collected data on 15 angular variables, suggested that "...a SD that falls in the lowest one-third of... all 15 angular SDs..." may be taken to indicate angular invariance. But this seems rather arbitrary—why the lowest one-third as opposed to the lowest one-quarter or one-half? Enlow and McNamara⁵, and later Enlow and Azuma⁶, implied that relative invariance is exhibited by angular measures characterized by a standard deviation of 6° or less (which is actually quite similar to the mark of 6.3° eventually adopted by Ravosa and Shea¹), although these authors give no justification for this particular cut-off point. Ravosa and Shea¹ reported a

mean of 90° and a standard deviation (SD) of 12.37° for the midfacial-cribriform angle in a sample of cercopithecoid monkeys (n=79). These authors argued that this magnitude of variance was too great to indicate angular invariance, or act as a constraint on craniofacial growth.

In fact, Ravosa and Shea¹ used two distinct sets of landmarks to identify the cribriform plate, which they called (A) and (B). They define cribriform plate (A) as a “line connecting the anteriormost and posteriormost aspects of the cribriform plate at the ethmoid/nasal cavity junction,” and (B) was taken as the “line connecting the anteriormost and posteriormost aspects of the cribriform plate at the anterior cranial base” (p. 819). For comparison, we used the data for their cribriform plate/midfacial angle (A), which appears to correspond closest to Enlow’s original definition. They report a smaller standard deviation (9.84°) for their cribriform plate/midfacial plane (B) measurement. The authors justify the use of the two separate measures “...so as to represent variation adequately in this region... especially since Enlow did not specify to which portions of the cribriform plate a plane must be fit” (p. 819). Two points must be made. First, Enlow and McNamara⁵ specified precisely and in great detail how a plane should be fit to the cribriform plate. They provided photographs of midsagittally sectioned skulls, lateral radiographs, and headfilm tracings, each with arrows or other markers indicating the precise locations of the landmarks used to define the cribriform plate (e.g., *ibid.*, Figs. 4, 5 & 6). Extensive word descriptions are also given in numerous publications^{e.g. 5 (p. 256), 6 (p. 227), 7}. The second point is that there is no need to distinguish separate pairs of endpoints of the cribriform plate, one pair at the anterior cranial base and the other at the ethmoid/nasal cavity. The cribriform plate is a thin wafer of bone with distinct anterior and posterior ends. What Ravosa and Shea¹ might have mistaken for as a second pair of plate ends is likely the anteriormost and

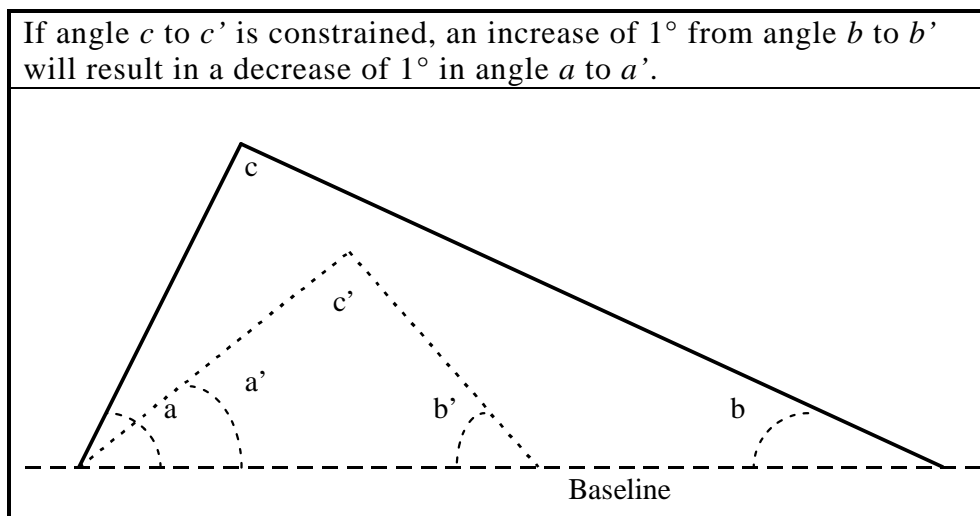
posteriormost junctions of the olfactory recess with the anterior cranial floor, and not the cribriform plate itself.

The Mean midfacial-cribriform angle computed for all 300 specimens amongst 37 species of anthropoids investigated by McMahon ⁸ is 89.3° (SD = 5.70; Regression co-efficient [95% CI] = -0.87 [95% CI, -0.93, -0.84]), which is not significantly different from the 90° degree angle reported by both Enlow and McNamara ⁵ and Ravosa and Shea ¹. The standard deviation for the entire sample was found to be 5.7°, similar to the value of 6° reported for a smaller but more diverse sample of mammals by Enlow and McNamara ⁵ but less than half the standard deviation reported by Ravosa and Shea ¹. The discrepancy between studies may be due to dissimilar measurement techniques. In both the investigations by McMahon ⁸ and that of Enlow and McNamara ⁵ some form of labeling technique was used to aid in the identification of the cribriform plate (brass filings and lead markers, respectively). Ravosa and Shea ¹ used no such method, a shortcoming that may have introduced measurement error into the data. High measurement error, if random, will not affect the mean, but it will lead to overestimated measures of dispersion (such as standard deviation), a pattern consistent with Ravosa and Shea's reported results.

To test for angular invariance due to constraint, a more biologically and analytically valid approach is to ask the question: Is the degree of angular variability low enough to produce a coordinated effect between the two planes whose intersection forms the angle in question? A given angle is invariant, or more correctly 'constrained,' if each of the two arms forming the angle, measured against a common reference plane, yields a regression coefficient significantly different from zero (assuming that the two arm-to-reference plane angles exhibit sufficient variance). For example, a 'perfect' constraint will be manifest as a constant angle, and in such

cases the slope of the regression between the two arms (each measured in degrees from a common baseline) will be equal to -1.0 because each increase of 1° in one arm will translate to a decrease of 1° in the other. This is shown diagrammatically in Appendix B Figure 1: if angle c to c' is constrained, then as the complex rotates (solid to dotted lines), for every 1° increase in angle b to b' there will be a corresponding 1° decrease in angle a to a' . Empirical regression slopes, measured in the manner described, that are not significantly different from -1.0 indicate a perfect constraint-mediated interdependence between the arms forming the angle in question, and this interdependence is manifested as angular invariance.

Appendix B, Figure 1



REFERENCES

1. Ravosa M.J. and Shea B.T. Pattern in craniofacial biology: evidence from the Old World monkeys (Cercopithecidae). *International Journal of Primatology*. 15: 801-821, 1994.
2. Pearson K. *Karl Pearson's Early Statistical Papers*. Cambridge University Press, Cambridge; 1956.

3. Simpson G.G., Roe A. and Lewontin R.C. Quantitative zoology, revised edn. Harcourt, Brace & World, New York; 1960.
4. Zingesser M.R. Occlusofacial morphological integration (*Homo sapiens*, *Alouatta caraya*, *Cebus capucinus*). In: Zingesser M.R., editor. Symposia of the Fourth International Congress of Primatology. Vol. 3: Craniofacial Biology of Primates. Karger, Basel. 241-257, 1973.
5. Enlow D.H. and McNamara J.A. The neurocranial basis for facial form and pattern. *Angle Orthod* 43: 256-270, 1973.
6. Enlow D.H. and Azuma M. Functional growth boundaries in the human and mammalian face. In: Langman J., editor. Morphogenesis and malformations of the face and brain. The National Foundation, New York; 217-230, 1975.
7. Enlow D.H. Handbook of facial growth. WB Saunders, Philadelphia; 1975.
8. McMahon J.M. Dissertation: Nomological mechanisms of anthropoid nasomaxillary diversity. City University of New York, New York; 1999.

Appendix C

Regression and non-parametric association of facial prognathism on relative endocranial volume. Data were adjusted for phylogenetic clustering using phylogenetic autocorrelation. Endocranial volume isometrically size scaled on cranial centroid size. (N = 300; across 37 species of anthropoids.)

Regression and non-parametric association of facial prognathism on relative endocranial volume		
Taxon	Maximum likelihood regression coefficients (95% CI) and associated p-value	Somers' D nonparametric test of association
Anthropoids (n=300)	-1.59 (-1.78, -1.40) p = .0001	-0.35 p < .05
Platyrrhini (n=117)	-2.46 (-1.95, -2.45) p = .0001	-0.34 p < .05
Atelidae (n=65)	-3.22 (-3.82, -2.61) p = .0001	-0.44 p < .05
Cebidae (n=52)	-1.88 (-2.67, -1.08) p = .0001	-0.35 p < .05
Catarrhini (n=183)	-1.57 (-1.76, -1.38) p = .0001	-0.48 p < .05
Cercopithecoidea (n=137)	-1.82 (-2.21, -1.41) p = .0001	-0.45 p < .05
Cercopithecinae (n=87)	-1.46 (-1.88, -1.02) p = .0001	-0.42 p < .05
Colobinae (n=50)	-3.28 (-4.13, -2.43) p = .0001	-0.50 p < .05
Hominoidea (n=46)	-1.51 (-1.78, -1.23) p = .0001	-0.43 p < .05

EDITORIAL

Is Physical Anthropology related to Craniofacial growth?

Although it is uncommon to include anthropological articles in the JCPD, it is not unusual to find new paradigms, philosophies, or concepts that can be extrapolated from another art or science into dentistry. In this particular case, Dr. Bromage and colleagues, using Dr. Enlow's concepts of growth and development, common to Pediatric Dentistry, Orthopedics and Orthodontics, clearly demonstrates that a new, more flexible approach to a basic concept can translate into different and more appropriate results.

In bolded print, we hope to elucidate some possibilities of knowledge extrapolation into both, clinical and scientific dentistry.

Dr. Tim Bromage and colleagues were motivated to perform this study because in the absence of biological criteria our preconceptions are likely to govern our concept of craniofacial form. Therefore, the authors reassembled the KNM-ER1470 fragmented parts - left and right halves of the calvaria and the face - according to mammalian craniofacial architectural constraints described by Donald H. Enlow and colleagues. When evaluated on a biological premise, KNM-ER 1470 is found to have a more prognathic midface than commonly appreciated.

An effort to reconstruct the skull was first made possible using biological principles that deriving from a series of investigations by Donald H. Enlow and colleagues from the 1960's to 1980's. Functional anatomical boundaries of the craniofacial skeleton in humans and mammalian species were found to be characterized by important growth sites and the relative placement of neural and pharyngeal compartments.

This finding alone, stresses the importance of airway consideration in today's diagnosis and treatment planning of orthopedic and orthodontic patients.

In this research, histological interpretations of human facial bone growth remodeling were explicitly combined with serial radiographic data in order to promote a new cephalometric system. Enlow and Hunter championed this new technique and outlined a series of anatomical parts and counterparts, which could be evaluated on the basis of growth equivalents and growth compensations between them.

A procedure was developed to explain how a pattern was produced as opposed to systems of cephalometric evaluation, which explained what craniofacial pattern resulted from growth. This course of action is important in the history of developing architectural concepts because it

explicitly linked dynamic growth processes to anatomical compartments and resultant craniofacial design. This process was more sensitive than traditional cephalometric methods exploring basicranial relations to craniofacial variability. This is because "an angular value such as Basion-Sella-Nasion is based on midline points, none of which are involved in the actual articular fitting of basicranium, maxilla, and mandible to each other, or in the anatomic basis of bilateral positioning among the respective parts; nor do they represent growth sites directly participating in this three-part relationship"

The utilization of anatomical landmarks and counterparts of growth in this cephalometric system may have an advantage for prediction, especially because this technique allows explicitly for dynamic growth, a very much needed consideration when measuring or predicting growth in children.

The relationship between prognathism and cranial capacity for fossil hominin and modern human and chimpanzee crania was examined by Thackeray and Monteith and measured by the formula described in this article.

Can a similar prediction formula for prognathism be applied to the growing Class III child? It would be of interest to both, the scientific and clinical communities, to correlate this formula with the prediction formulas used today.

A best fit covariance structural model confirmed the hypothesis of Enlow and McNamara that cribriform plate orientation is the primary mediator between the development and evolution of the brain and nasomaxillary morphology.

When a new finding corroborates a previous concept, the validity of such concept increases and, therefore, its use as an indicator or predictor is strengthened.

The problem a scientist or engineer chooses to solve and the way he breaks that problem or system down into components is a choice of his making; it is a function of among other things, his particular scientific technical training and his personality.

In short, what one observes is a basic function of what one has been trained to observe.

By retraining ourselves and using new technological advances we can broaden the horizon, which translates into providing optimal diagnosis and treatment for our patients.

Dr Denise Vedrenne
Associate Editor